Modeling the effect of upstream temperature fluctuations on shock/homogeneous turbulence interaction

Vijay K. Veera and Krishnendu Sinha[a)]
Department of Aerospace Engineering, Indian Institute of Technology Bombay, Mumbai 400076, India

(Received 23 April 2008; accepted 23 December 2008; published online 4 February 2009)

Reynolds-averaged Navier–Stokes (RANS) equations can yield significant error when applied to the interaction of turbulence with shock waves. This is often due to the fact that RANS turbulence models do not account for the underlying physical phenomena correctly. For example, in the presence of appreciable temperature fluctuations in the upstream flow, turbulence amplification across a shock is significantly affected by the magnitude of the temperature fluctuations and the sign of the upstream velocity-temperature correlation [Mahesh *et al.*, J. Fluid Mech. **334**, 353 (1997)]. Standard two-equation models with compressibility correction do not reproduce this effect. We use the interaction of homogeneous isotropic turbulence with a normal shock to suggest improvements to the k-ϵ model. The approach is similar to that presented in an earlier work [Sinha *et al.*, Phys. Fluids **15**, 2290 (2003)]. Linear inviscid analysis is used to study the effect of upstream temperature fluctuations on the evolution of turbulent kinetic energy k across the shock. The dominant mechanisms contributing to the k amplification are identified and then modeled in a physically consistent way. The dissipation rate equation is also altered based on linear analysis results. The modifications yield significant improvement over existing two-equation models and the new model predictions are found to match linear theory and direct numerical simulation data well. © *2009 American Institute of Physics*. [DOI: 10.1063/1.3073744]

I. INTRODUCTION

In high-speed aerospace vehicles, shock waves generated by different parts of the body can interact with and severely alter the turbulent boundary layer on the surface. Typical effects include flow separation, pressure rise, and enhancement of heat transfer, which are often important factors in vehicle design. Interaction of the turbulent fluctuations in the boundary layer with the shock wave is one of the basic phenomena in these flows. Understanding and accurate prediction of shock/turbulence interaction are therefore critical in achieving reliable prediction capability.

Reynolds-averaged Navier–Stokes (RANS) simulations are generally used for engineering applications, but their performance in shock dominated flows is often limited by the accuracy of the underlying turbulence model.[1] Some attempts have been made to improve model predictions, e.g., realizability constraint,[2] compressibility correction,[3,4] length scale modification,[4] and rapid compression correction.[4] The outcome of the modifications varies from model to model and with the test conditions, which point to the possibility that some key physical processes are either modeled incorrectly or not included in the models.

The interaction of homogeneous isotropic turbulence with a normal shock is a fundamental problem for which direct numerical simulation (DNS) and linear analysis solutions exist. It is therefore an ideal problem for identifying the physical mechanisms underlying shock/turbulence interactions. Sinha *et al.*[5] used the RANS equations to study shock/homogeneous turbulence interaction. It is found that the standard k-ϵ model grossly overpredicts the amplification in turbulent kinetic energy k across the shock. This is attributed to the fact that the underlying eddy viscosity assumption breaks down in a rapidly distorting mean flow. Modifications based on suppressing the eddy viscosity in a shock wave yield a lower amplification in k, but the predictions are still higher than DNS. Based on a detailed analysis of the governing equations, they identify a damping mechanism due to unsteady shock motion and model it using linear analysis. The resulting equation matches DNS data of shock/homogeneous turbulence interaction well. Application of the shock-unsteadiness model to canonical flows such as compression corner[6] and oblique shock impingement problem[7] shows appreciable improvement.

The analysis in Ref. 5 assumes that the turbulence upstream of the shock is composed of vortical fluctuations, i.e., the effect of entropic and acoustic components is neglected. However, experimental[8] and DNS (Ref. 9) data suggest that practical flows in the supersonic regime, such as constant pressure boundary layers, have the entropy field and the vortical fluctuations of comparable magnitude. As per Morkovin's hypothesis, turbulent fluctuations in a compressible boundary layer are essentially composed of vorticity and entropy modes, i.e., the acoustic mode is negligible. Fluctuations in total temperature are also assumed to be negligible, which results in the following relation between the thermodynamic and velocity fields:

[a)]Author to whom correspondence should be addressed. Electronic mail: krish@aero.iitb.ac.in.

$$\frac{\rho'}{\bar{\rho}} = -\frac{T'}{\bar{T}} = (\gamma - 1)M^2\frac{u'}{\bar{u}}, \tag{1}$$

where ρ, T, and u are the density, temperature, and streamwise velocity and M is the mean flow Mach number. Overbar represents Reynolds averaging, while prime indicates the fluctuating part.

Mahesh *et al.*[10] found that the presence of upstream entropy fluctuations significantly affects shock/turbulence interactions. A negative correlation between the upstream velocity and temperature fluctuations is found to cause higher levels of turbulence amplification across the shock, whereas a positive correlation is seen to have the opposite effect. In this paper, we study the effect of upstream velocity-temperature correlation on the amplification of k in the RANS framework. The objective is to use linear inviscid analysis to improve model predictions in the presence of temperature fluctuations in the incoming turbulent flow.

The paper is organized as follows. A comprehensive statement of the problem is given in the next section. This is followed by an analysis of the governing equation for turbulent kinetic energy across a shock wave. The source term corresponding to the production mechanism due to the mean pressure gradient is found to be the dominant mechanism through which the velocity-temperature correlation affects k amplification across the shock. A model is then developed for this term using linear analysis results. The dissipation rate equation is also modified in a similar way. The resulting model is finally applied to predict the evolution of turbulent kinetic energy in shock/homogeneous turbulence interaction, and results are compared with the available DNS data.

II. PROBLEM DESCRIPTION

We consider uniform mean flow upstream and downstream of a normal shock. The shock wave is steady in the mean and undergoes small deviations from its mean position in response to the turbulent fluctuations. The turbulence upstream of the shock is assumed to be homogeneous and isotropic, with the thermodynamic field related to the velocity fluctuations by

$$\frac{\rho'}{\bar{\rho}} = -\frac{T'}{\bar{T}} = A_{uT}\frac{u'}{\bar{u}}. \tag{2}$$

Here, the acoustic fluctuations are neglected $(p'=0)$ and Morkovin's hypothesis is satisfied for $A_{uT}=(\gamma-1)M^2$. A_{uT} can be interpreted as the ratio of normalized temperature and velocity fluctuations, and it can be readily seen that

$$\frac{\overline{u'T'}}{\bar{u}\bar{T}} = -A_{uT}\frac{\overline{u'^2}}{\bar{u}^2}. \tag{3}$$

We choose constant values of A_{uT} and study the effect of $\overline{u'T'}$ on the amplification in k across a normal shock as a function of the upstream Mach number. Both positive and negative values of A_{uT} are considered, which correspond to $\overline{u'T'}<0$ and $\overline{u'T'}>0$, respectively. A quadratic variation of A_{uT} with Mach number that is consistent with Morkovin's hypothesis, Eq. (1), is also presented.

Mahesh *et al.*[11] considered the interaction of vorticity-entropy waves with a normal shock. The ratio of entropy to vorticity magnitudes of each wave is defined as A_r and the phase difference is given by ϕ_r. It can be shown that $A_r e^{i\phi_r} = A_{uT}\sin\psi$, where ψ is the angle made by the wave number vector with the shock-normal direction. Thus $\phi_r=0$ for the positive A_{uT} values considered in this work, while negative A_{uT} values correspond to $\phi_r=\pi$. In both cases, the $\sin\psi$ functional dependence results in an axisymmetric entropy field for an isotropic vortical flow.

III. TRANSPORT EQUATION FOR *k*

For turbulent fluctuations passing through a normal shock wave, the unsteady distortion of the shock from its mean position can be written as $x=\xi(y,z,t)$, where x is the shock-normal direction. To account for the shock-unsteadiness effects, Sinha *et al.*[5] derived a transport equation for k in the frame of reference attached to the instantaneous shock wave. The key results are reproduced below for the sake of completeness.

Assuming that the shock undergoes small deviations from its mean position, the linearized momentum conservation equation is written in the frame of reference that is attached to the shock. This equation is then used to derive the following transport equation for $\widetilde{u''^2}$:

$$\bar{\rho}\tilde{u}\frac{\partial}{\partial x}\frac{\widetilde{u''^2}}{2} = -\bar{\rho}\widetilde{u''^2}\frac{\partial\tilde{u}}{\partial x} + \bar{\rho}\widetilde{u''\xi_t}\frac{\partial\tilde{u}}{\partial x} - \overline{u''}\frac{\partial\bar{p}}{\partial x} - \overline{u'p'_{,x}}, \tag{4}$$

where p is pressure and ξ_t is the linear velocity of the shock in the streamwise direction. Tilde represents Favre averaging, with double prime being Favre fluctuations. Note that higher order and viscous terms are neglected in the vicinity of the shock wave.

The source terms on the right hand side are identified as the production due to mean compression, the shock-unsteadiness term, the production due to mean pressure gradient, and the pressure-velocity term. These are denoted by P_k, S_k^1, Π_k^3, and Π_k^1, respectively. The production due to mean pressure gradient can be written as

$$\Pi_k^3 = -\overline{u''}\frac{\partial\bar{p}}{\partial x} = \frac{\overline{\rho'u'}}{\bar{\rho}}\frac{\partial\bar{p}}{\partial x} = \frac{\overline{u'T'}}{\bar{T}}\bar{\rho}\tilde{u}\frac{\partial\tilde{u}}{\partial x}, \tag{5}$$

where $\rho'/\bar{\rho}=-T'/\bar{T}$ is based on the assumption that pressure fluctuations are negligible in the inflow turbulence. Note that negatively correlated velocity and temperature fluctuations $(\overline{u'T'}<0)$ result in a positive source term, thus enhancing the amplification of $\widetilde{u''^2}$. On the other hand, a positive $\overline{u'T'}$ correlation has a damping effect on $\widetilde{u''^2}$. This is identical to the trend observed in linear analysis[11] and DNSs.[10,12]

A similar transport equation is derived for the transverse velocity fluctuations $\widetilde{v''^2}$,

$$\bar{\rho}\tilde{u}\frac{\partial}{\partial x}\frac{\widetilde{v''^2}}{2} = -\bar{\rho}\tilde{u}\widetilde{v''\xi_y}\frac{\partial \tilde{u}}{\partial x}, \tag{6}$$

where ξ_y is the angular distortion of the shock, and the source term due to shock distortion is denoted by S_k^2. Note that $\widetilde{w''^2}$ follows an equation similar to $\widetilde{v''^2}$.

The linearized Rankine–Hugoniot relations presented by Mahesh *et al.*[10] are used to write the following equations for the change in $\overline{u'^2}$ and $\overline{v'^2}$ across a shock:

$$\bar{\rho}_1\bar{u}_1\frac{1}{2}(\overline{u_2'^2} - \overline{u_1'^2}) = -\bar{\rho}_1\overline{u_1'u_m'}\Delta\bar{u} + \bar{\rho}_1\overline{u_m'\xi_t}\Delta\bar{u} + \frac{\overline{u_m'T_1'}}{\bar{T}_1}\bar{\rho}_1\bar{u}_1\Delta\bar{u} - \overline{u_m'(p_2' - p_1')}, \tag{7}$$

$$\bar{\rho}_1\bar{u}_1\tfrac{1}{2}(\overline{v_2'^2} - \overline{v_1'^2}) = -\bar{\rho}_1\bar{u}_1\overline{\tfrac{1}{2}(v_1' + v_2')\xi_y}\Delta\bar{u}, \tag{8}$$

where $u_m' = (u_1' + u_2')/2$ and $\Delta\bar{u} = (\bar{u}_2 - \bar{u}_1)$; subscripts 1 and 2 denote shock upstream and downstream locations. The above equations can be interpreted as integrated forms of Eqs. (4) and (6), with one-to-one correspondence between the terms on the left and right hand sides. Note that $u'' = u'$ and $\tilde{u} = \bar{u}$ in the linear limit.

Figure 1 shows the budget of the above equations as a function of the upstream Mach number M_1. The data (normalized by $\bar{\rho}_1\bar{u}_1^3$) are presented for different A_{uT} values. $A_{uT} = 0$ corresponds to purely vortical turbulence upstream of the shock. Positive values of A_{uT} (0.58, 1.0, 2.0, and 4.0) are chosen for detailed analysis and model development. Negative A_{uT} and a quadratic variation of A_{uT} with Mach number are subsequently discussed. Note that the $A_{uT} = 0.58$ case was analyzed by Mahesh *et al.*[11]

The budget of source terms for $A_{uT} = 0$ [Fig. 1(a)] is identical to that presented in Ref. 5. The production due to mean compression amplifies turbulence, while the shock-unsteadiness term reduces $\widetilde{u''^2}$. The pressure-velocity term is negative except at low Mach numbers, whereas the shock-distortion mechanism is found to amplify k. The production due to mean pressure gradient is identically zero for this case. As expected, Π_k^3 has an amplifying effect on $\widetilde{u''^2}$ for $A_{uT} > 0$. Its magnitude increases rapidly with A_{uT} to become one of the dominant effects at $A_{uT} = 2$ and above. By comparison, the production due to mean compression is relatively unchanged across the range of A_{uT} considered. The remaining source terms retain their qualitative variation with Mach number, but their magnitude is enhanced progressively as A_{uT} increases.

The turbulent kinetic energy shows a rapid nonmonotonic variation behind the shock. Mahesh *et al.*[11] explained this variation by noting that

$$\frac{\gamma M}{2}\left[\frac{2k}{\tilde{a}^2} + \frac{\overline{p'^2}}{\gamma^2\bar{p}^2}\right] + \frac{\overline{p'u'}}{\bar{p}\tilde{a}} = \text{const} \tag{9}$$

downstream of the shock wave. The interaction of vortical and entropy waves with a shock generates acoustic energy, i.e., $\overline{p'^2} \neq 0$ and $\overline{p'u'} \neq 0$ immediately downstream of the shock. Majority of the acoustic energy decays rapidly and is transferred to the kinetic form as per the above equation. The change in k due to this energy transfer mechanism is denoted by a source term, Π_k^2, in the k equation, and the total contribution of this term is plotted as a function of Mach number for different A_{uT} values in Fig. 1.

The different mechanisms discussed above can be combined with the viscous dissipation rate ϵ to get an equation for the turbulent kinetic energy $k = (\widetilde{u''^2} + \widetilde{v''^2} + \widetilde{w''^2})/2$. Thus,

$$\bar{\rho}\tilde{u}\frac{\partial k}{\partial x} = P_k + S_k^1 + 2S_k^2 + \Pi_k^1 + \Pi_k^2 + \Pi_k^3 - \bar{\rho}\epsilon \tag{10}$$

governs the interaction of homogeneous isotropic turbulence with a normal shock. A factor of 2 multiplies S_k^2 in order to include the shock-distortion effects on $\widetilde{w''^2}$.

IV. MODELING

Grasso and Falconi[13] presented a model for the production due to mean pressure gradient, where the Favre velocity fluctuations are modeled in terms of the mean density gradient,

$$\Pi_k^3 = -\frac{\mu_T}{\bar{\rho}^2}\frac{1}{\sigma_\rho}\frac{\partial\bar{\rho}}{\partial x_j}\frac{\partial\bar{p}}{\partial x_j}. \tag{11}$$

Here μ_T is the turbulent eddy viscosity, σ_ρ is 0.5, and subscript $j = 1, 2, 3$ represents the three spatial directions. When applied to the evolution of homogeneous turbulence through a normal shock, this term has a damping effect on k, since the gradients of mean density and pressure are positive across the shock. Thus, the model does not reproduce the amplifying effect of upstream entropy fluctuations when the velocity-temperature correlation is negative. Because of this nonphysical behavior, we do not pursue the above model further. Instead we develop an alternate model for Π_k^3.

The production due to mean pressure gradient is a function of $\overline{u'T'}/\bar{T}$. For a given A_{uT}, $\overline{u'T'}$ can be assumed to be proportional to the streamwise velocity fluctuations in the upstream turbulence (see Sec. II). Using Eq. (3) therefore results in

$$\Pi_k^3 = \frac{\overline{u'T'}}{\bar{T}}\bar{\rho}\tilde{u}\frac{\partial\tilde{u}}{\partial x} = -A_{uT}\bar{\rho}\widetilde{u''^2}\frac{\partial\tilde{u}}{\partial x}. \tag{12}$$

Sinha *et al.*[5] modeled the shock-unsteadiness term as

$$S_k^1 = \bar{\rho}\widetilde{u''^2}\frac{\partial\tilde{u}}{\partial x}b_1, \tag{13}$$

where the modeling coefficient b_1 is obtained as a curve fit to the ratio $\overline{u_1'\xi_t}/\overline{u_1'^2}$. Values of this ratio are computed using linear analysis for different cases of A_{uT} and are plotted as a function of Mach number in Fig. 2. The $A_{uT} = 0$ case is once again identical to that presented earlier.[5] For $A_{uT} > 0$, the effect of incident temperature fluctuations is to amplify the unsteady shock motion, such that $\overline{u_1'\xi_t}$ exceeds incident velocity fluctuations for high values of A_{uT}. In all cases, b_1 asymptotes to a limiting value as $M_1 \to \infty$. The asymptotic value $b_{1,\infty}$ increases linearly with A_{uT} (see Fig. 3), and the variation is closely approximated by

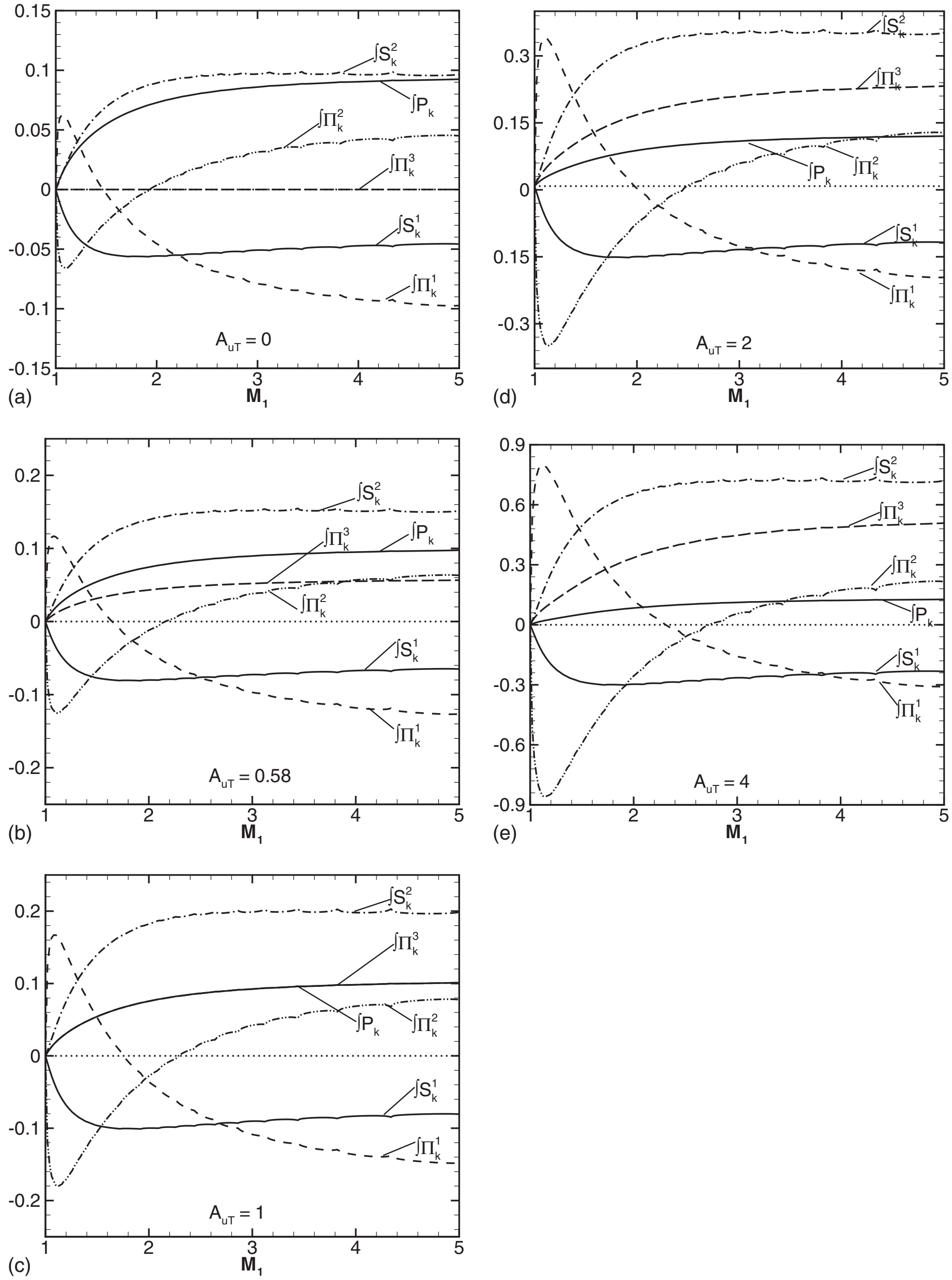

FIG. 1. Budget of Eqs. (7) and (8) as a function of upstream Mach number for different values of A_{uT}. P_k=production due to mean compression, S_k^1=shock-unsteadiness term, S_k^2=shock distortion term, Π_k^1=pressure-velocity term, Π_k^3=production due to mean pressure gradient, and $\int$ represents the integration across the shock. $\int\Pi_k^2$ is the total contribution of the energy exchange mechanism downstream of the shock. All terms are normalized by $\bar{\rho}_1\tilde{u}_1^3$.

$$b_{1,\infty} = 0.4 + 0.2A_{uT}. \tag{14}$$

The other terms S_k^2, Π_k^1, and Π_k^2 are modeled in Ref. 5 by modifying the coefficient b_1 to

$$b_1' = b_{1,\infty}(1 - e^{1-M_1}). \tag{15}$$

The same form is retained here with $b_{1,\infty}$ given above as a function of A_{uT}.

Introducing these models into Eq. (10) we get

$$\bar{\rho}\tilde{u}\frac{\partial k}{\partial x} = -\bar{\rho}\widetilde{u''^2}(1 - b_1' + A_{uT})\frac{\partial \tilde{u}}{\partial x} - \bar{\rho}\epsilon. \tag{16}$$

Using the isotropic form of Reynolds stress, $\widetilde{u''^2}=2k/3$ (by setting $\mu_T=0$ as in Ref. 5) and neglecting the viscous dissipation results in the following closed form solution for k amplification across the shock:

$$\frac{k_2}{k_1} = \left(\frac{\tilde{u}_1}{\tilde{u}_2}\right)^{(2/3)(1-b_1'+A_{uT})}. \tag{17}$$

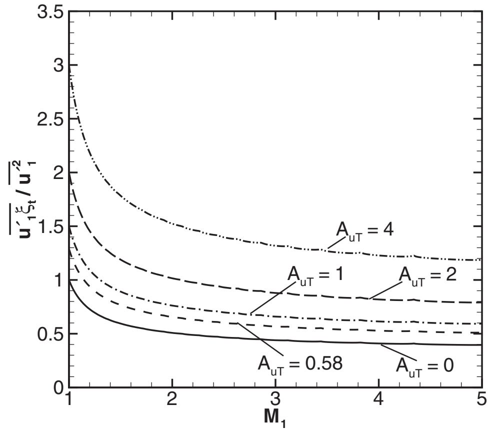

FIG. 2. The ratio $\overline{u_1'\xi_t}/\overline{u_1'^2}$ computed from linear analysis (Ref. 11) as a function of upstream Mach number for different values of A_{uT}.

As per Boussinesq approximation, the Reynolds stress $\widetilde{u''^2}$ is given by[14]

$$\widetilde{u''^2} = -\frac{4}{3}\mu_T\frac{\partial\tilde{u}}{\partial x} + \frac{2}{3}\bar{\rho}k. \tag{18}$$

On substitution in the modeled k equation (16), it results in a source term that is proportional to $(\partial\tilde{u}/\partial x)^2$. At a shock wave, the source term assumes very large values ($\propto 1/\delta^2$, where δ is the mean shock thickness). This leads to very high amplification of turbulent kinetic energy. As discussed in Ref. 5, the production term in the standard k-ϵ model exhibits its identical trend, and the amplification of k increases rapidly as the computational grid is refined to get a thinner shock.[5] It is argued that this nonphysical behavior of the k equation is primarily caused by the breakdown of the eddy viscosity assumption in a highly nonequilibrium flow such as a shock wave. One means to avoid this trend is to suppress eddy viscosity in the region of rapid compression. Setting $\mu_T=0$ in the shock wave thus results in the isotropic form of the Reynolds stress, which is used to obtain the k amplification given in Eq. (17).

Figure 4 compares the model predictions with linear analysis results. For $A_{uT}=0$ the above equation is identical to

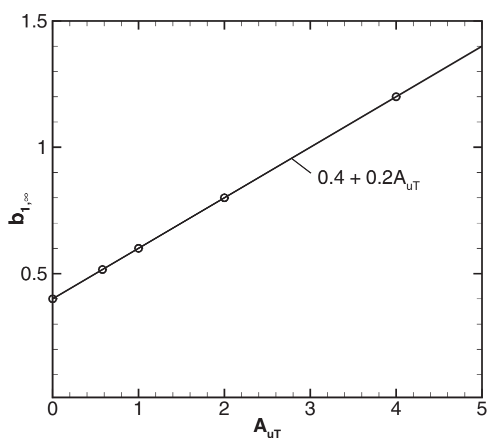

FIG. 3. Variation of the high Mach number limiting value of b_1 as a function of A_{uT}.

the model presented in Ref. 5 and compares well with the linear theory results. For $A_{uT}>0$, the model matches the theoretical values only at low Mach numbers and overpredicts the amplification in k at higher Mach numbers. The magnitude of overprediction rapidly increases with the level of temperature fluctuations in the upstream flow. Results obtained for $A_{uT}=0$ using a realizable k-ϵ model and by setting $\mu_T=0$ are reproduced from Ref. 5. These models significantly overpredict the amplification in k at higher Mach numbers, and the model predictions are insensitive to upstream temperature fluctuations. They are therefore omitted from $A_{uT}>0$ plots.

Next, we attempt to improve the modeling of Π_k^3. Instead of using the upstream value of $\overline{u'T'}/\bar{T}$ given by Eq. (3), taking the average of upstream and downstream quantities may give a better estimate of $\overline{u'T'}/\bar{T}$,

$$\frac{\overline{u'T'}}{\bar{T}} \simeq \frac{1}{2}\left[\frac{\overline{u_1'T_1'}}{\bar{T}_1} + \frac{\overline{u_2'T_2'}}{\bar{T}_2}\right] = \frac{1}{2}\frac{\overline{u_1'T_1'}}{\bar{T}_1}\left[1 + \frac{\overline{u_2'T_2'}}{\overline{u_1'T_1'}}\frac{\bar{T}_1}{\bar{T}_2}\right]. \tag{19}$$

The ratio of the correlations $\overline{u_2'T_2'}/\overline{u_1'T_1'}$ is computed from linear analysis and plotted in Fig. 5 as a function of M_1 and A_{uT}. The ratio is of the order unity except for high Mach numbers, especially at low values of A_{uT} (for example, $A_{uT}=0.58$). As a first approximation we assume $\overline{u_2'T_2'} \sim \overline{u_1'T_1'}$. The limitations and justifications of this assumption in the $A_{uT} \to 0$ limit are described below. Thus,

$$\frac{\overline{u'T'}}{\bar{T}} \simeq \frac{1}{2}\frac{\overline{u_1'T_1'}}{\bar{T}_1}\left[1 + \frac{\bar{T}_1}{\bar{T}_2}\right] \simeq -\frac{A_{uT}}{2}\left(1 + \frac{\bar{T}_1}{\bar{T}_2}\right)\frac{\widetilde{u''^2}}{\tilde{u}}, \tag{20}$$

where Eq. (3) is used to arrive at the final form of the modeled term. The mean temperature ratio across the shock is close to 1 at low Mach numbers, and the new model approaches Eq. (12). At higher Mach numbers $\bar{T}_1/\bar{T}_2<1$. Hence the above model is expected to yield improved predictions than Eq. (12) by reducing the amplifying effect of Π_k^3. Incorporating this model gives the final form of the k equation,

$$\bar{\rho}\tilde{u}_i\frac{\partial k}{\partial x_i} = -\frac{2}{3}\bar{\rho}kS_{jj}\left[1 - b_1' + \frac{A_{uT}}{2}\left(1 + \frac{1}{T_r}\right)\right] - \bar{\rho}\epsilon, \tag{21}$$

where $T_r=\bar{T}_2/\bar{T}_1$ is the mean temperature ratio across the shock and is a function of upstream Mach number. $S_{jj}=\partial\tilde{u}_j/\partial x_j$ is the mean dilatation and is used to write the frame-independent form of the equation.

Integration of the above equation across the shock (with $\epsilon=0$) yields an amplification in k which has a form similar to Eq. (17) and is plotted in Fig. 4. The model results match Eq. (17) and linear theory for $A_{uT}=0$. The predictions also match theory within $\pm 10\%$ for $A_{uT}=0.58$, 1, and 2. At higher A_{uT}, the model is found to overpredict the theory. The $M_1\to\infty$ prediction of the model for varying A_{uT} is compared with the asymptotic linear theory results in Fig. 6. The model equation (21) yields accurate amplification in k up to $A_{uT}=3$, after which it deviates from the theoretical result. By comparison, Eq. (17) grossly overpredicts turbulence amplification except for very low levels of temperature fluctuations.

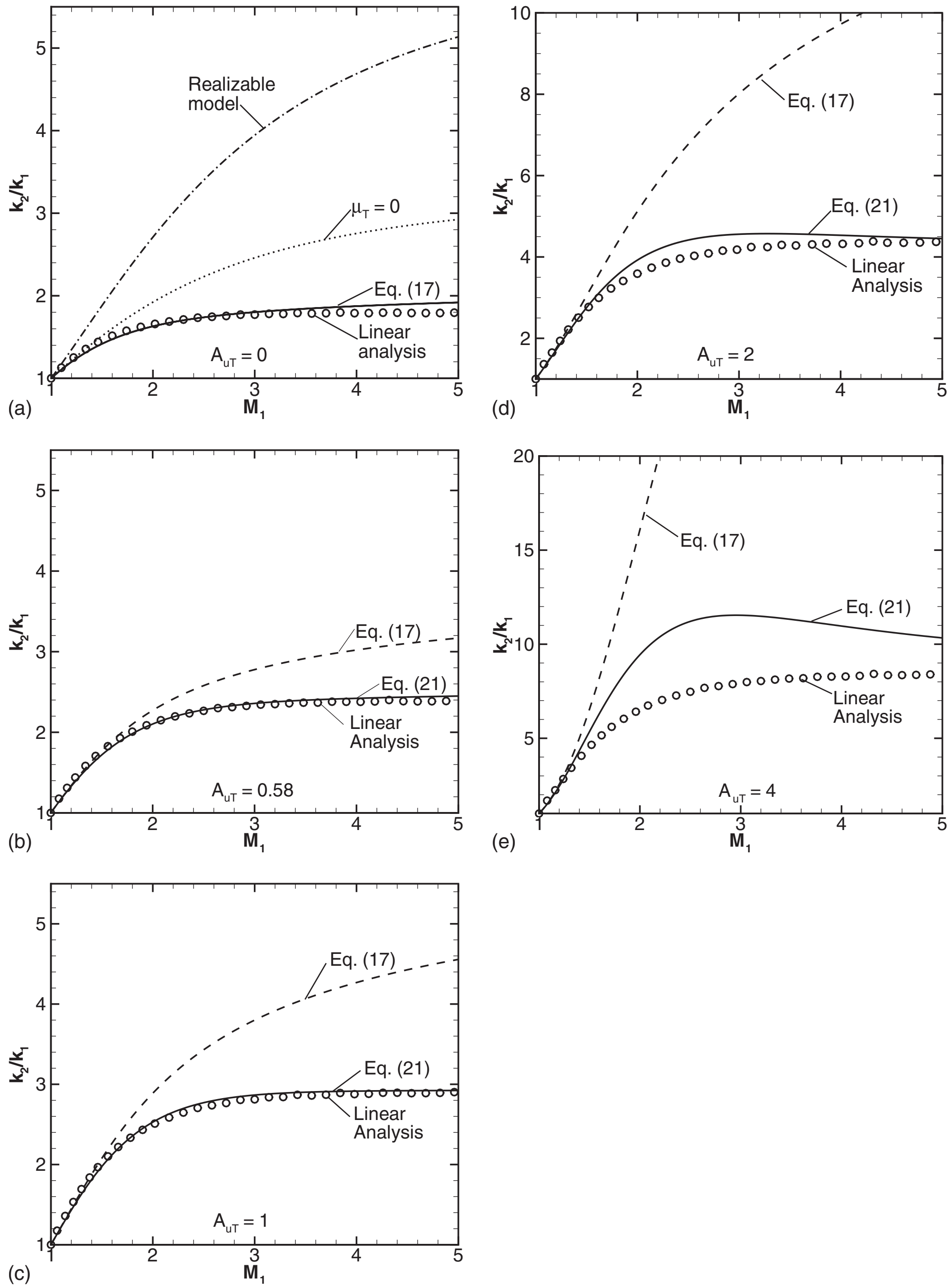

FIG. 4. Turbulent kinetic energy amplification in shock/homogeneous turbulence interaction as a function of the upstream Mach number for different values of A_{uT}. Two improvements to the k-ϵ model are compared to linear analysis (Ref. 11).

The above model is based on the assumption that $\overline{u_2'T_2'} \sim \overline{u_1'T_1'}$, which may not be valid in the limit $A_{uT} \to 0$. This is because the interaction of vortical turbulence with a shock wave produces entropy fluctuations behind the shock. As a result, $\overline{u_2'T_2'}$ may not be negligible for vanishingly small $\overline{u_1'T_1'}$ (when $A_{uT} \simeq 0$). However, at low A_{uT} the contribution of the Π_k^3 source term to the k budget is small compared to the production and shock-unsteadiness terms. The shock-unsteadiness model presented in Ref. 5 accounts for the dominant effects of P_k and S_k^1 and yields correct amplification in k when $A_{uT}=0$. In this limit, the current model collapses to the shock-unsteadiness model, such that the limitation in Π_k^3 modeling has negligible effect on the final result. This is corroborated by the close match between linear theory and model predictions in Fig. 6.

A. Upstream flow with negative A_{uT}

We study a negative A_{uT} case, which corresponds to a positive velocity-temperature correlation upstream of the shock. Following Mahesh *et al.*,[11] $A_{uT}=-0.58$ is used for the analysis. The main effect of negative A_{uT} is a negative Π_k^3 term in the budget of turbulent kinetic energy (see Fig. 7). The production term remains unchanged, and the other

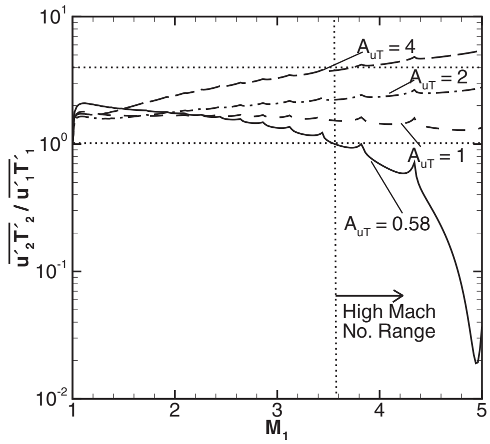

FIG. 5. The ratio of velocity-temperature correlation magnitude downstream and upstream of the shock, $\overline{u_2'T_2'}/\overline{u_1'T_1'}$, as a function of M_1 for different values of A_{uT}.

source terms S_k^1, S_k^2, Π_k^1, and Π_k^2 retain their qualitative variation with Mach number but are reduced in magnitude compared to the $A_{uT}=0$ case [Fig. 1(a)]. Negative Π_k^3 has a damping effect on the turbulent kinetic energy, which is consistent with the observations of Mahesh *et al.*[10] The model equation (21) is applied to this case with $b_{1,\infty}$ given by Eq. (14). The results presented in Fig. 8 show that the model matches linear theory within $\pm 10\%$ up to $M_1 \simeq 4$ and overpredicts the k amplification at higher Mach numbers. Comparison with the $A_{uT}=0$ case highlights the damping effect of negative A_{uT}. Note that Eq. (14) may be used only for $A_{uT}>-2$ for which $b_{1,\infty}>0$.

B. Upstream flow satisfying Morkovin's hypothesis

The thermodynamic and velocity fluctuations upstream of the shock satisfy Morkovin's hypothesis when $A_{uT}=(\gamma-1)M_1^2$. The model equation (21) is applied with $b_{1,\infty}=0.4+0.2(\gamma-1)M_1^2$ and the resulting k amplification is presented in Fig. 9. The model predictions are within 10% of linear analysis for Mach numbers up to 2.2, for which $A_{uT}\leq 2.0$. At higher Mach numbers, and therefore higher A_{uT}, the model overpredicts the amplification of turbulent kinetic energy across the shock. This is consistent with the trend observed for different A_{uT} cases presented in Fig. 4.

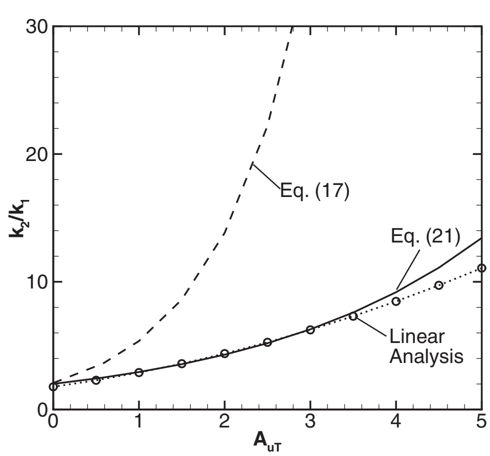

FIG. 6. Asymptotic ($M_1\to\infty$) model prediction for k amplification across a shock as a function of A_{uT}. Equations (17) and (21) are compared with the linear theory results.

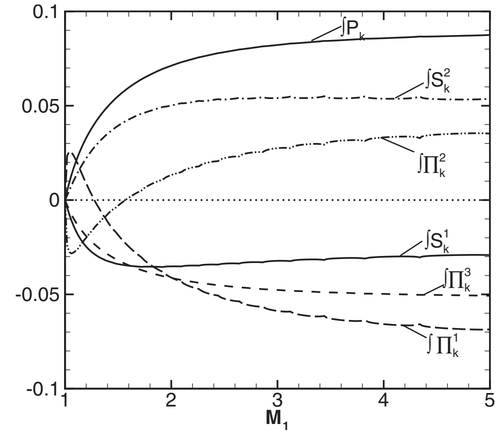

FIG. 7. Budget of Eqs. (7) and (8) at different Mach numbers for $A_{uT}=-0.58$ (see Fig. 1 for reference).

V. TURBULENT DISSIPATION RATE

The turbulent dissipation rate consists of a solenoidal part, a compressible part, and contributions due to inhomogeneity and fluctuations in viscosity. Sinha *et al.*[5] assumed that the solenoidal dissipation rate is the dominant dissipative mechanism. It is given by $\epsilon_s=\bar{\nu}\overline{\omega_i'\omega_i'}$, where $\bar{\nu}$ is the mean kinematic viscosity and ω_i' is the vorticity fluctuation.

The modeled transport equation for the solenoidal dissipation rate for one-dimensional mean flow through a normal shock is given by[14]

$$\bar{\rho}\tilde{u}\frac{\partial \epsilon_s}{\partial x} = -c_{\epsilon 1}\bar{\rho}\widetilde{u''^2}\frac{\partial \tilde{u}}{\partial x}\frac{\epsilon_s}{k} - c_{\epsilon 2}\frac{\epsilon_s^2}{k}, \tag{22}$$

where $c_{\epsilon 1}=1.35$ and $c_{\epsilon 2}=1.8$ are model constants.[15] The terms on the right hand side denote the production and dissipation mechanisms, respectively. The production term is dominant in a shock wave and can be integrated using the

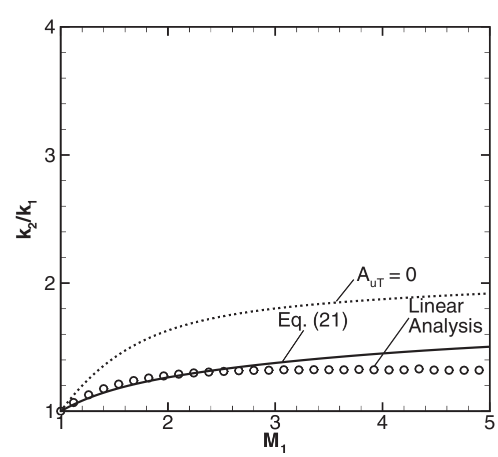

FIG. 8. Turbulent kinetic energy amplification predicted by Eq. (21) is compared with linear theory for different Mach numbers when $A_{uT}=-0.58$.

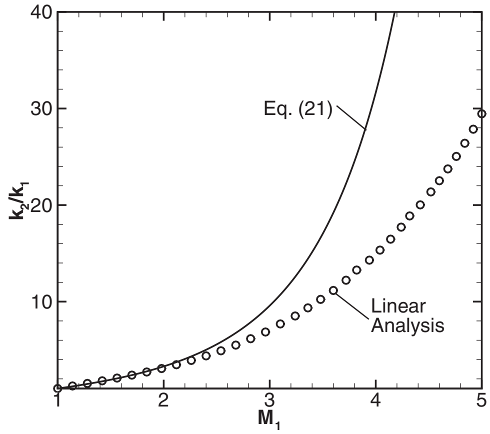

FIG. 9. Amplification of k predicted by Eq. (21) is compared with linear theory for different Mach numbers when $A_{uT}=(\gamma-1)M_1^2$.

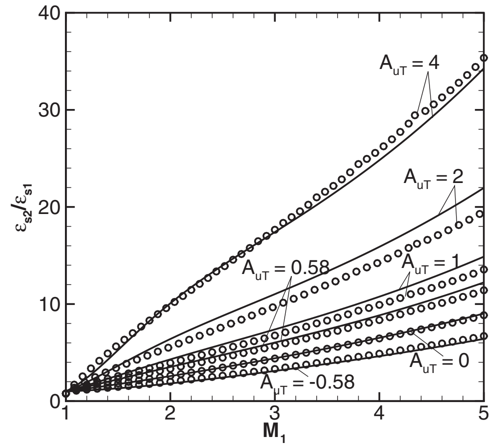

FIG. 10. Amplification in solenoidal dissipation rate in shock/homogeneous turbulence interaction as a function of the upstream Mach number. A curve fit for $c_{\epsilon 1}$ (lines) is obtained to match the linear theory predictions (symbols) for different A_{uT}.

isotropic form of the Reynolds stress $(\widetilde{u''^2}=2k/3)$. The resulting amplification in ϵ_s across the shock is

$$\frac{\epsilon_{s2}}{\epsilon_{s1}} = \left(\frac{\tilde{u}_1}{\tilde{u}_2}\right)^{(2/3)c_{\epsilon 1}}. \tag{23}$$

In the absence of upstream temperature fluctuations, Sinha *et al.*[5] proposed the following form of $c_{\epsilon 1}$ to match linear theory prediction for ϵ_s amplification across the shock,

$$c_{\epsilon 1} = 1.25 + 0.2(M_1 - 1). \tag{24}$$

The resulting model matches well with DNS data for shock/isotropic turbulence interaction.

We study the effect of $\overline{u'T'}$ correlation on ϵ_s amplification. The incident velocity-temperature correlation is shown to affect the amplification of vorticity fluctuations in the same way as turbulent kinetic energy.[10] $\overline{u'T'}<0$ enhances the vorticity amplification and $\overline{u'T'}>0$ has the opposite effect. Linear analysis is used to compute the amplification in ϵ_s across the shock as a function of upstream Mach number for different values of A_{uT}, and the results are plotted in Fig. 10. Following the approach in Ref. 5, we modify the coefficient $c_{\epsilon 1}$ to incorporate the effect of velocity-temperature correlation such that $\epsilon_{s2}/\epsilon_{s1}$ given by Eq. (23) matches linear theory results.

$$c_{\epsilon 1} = [1.25 + 0.2(M_1 - 1)] + A_{uT}(1 - 0.1A_{uT})(0.5 + e^{1-M_1}), \tag{25}$$

where the first part is identical to the $A_{uT}=0$ case given above, and the second part brings in the effect of velocity-temperature correlation. For $A_{uT}<10$, positive A_{uT} increases $c_{\epsilon 1}$ and thus enhances ϵ_s amplification, and negative A_{uT} has a damping effect on the dissipation rate. As shown in Fig. 10, the above model reproduces linear theory results for $1 \le M \le 5$ and $-0.58 \le A_{uT} \le 4$ reasonably well. A more rigorous approach would be to identify and model the physical mechanisms that affect ϵ_s amplification across the shock. Such an analysis is beyond the scope of the current paper.

Note that the modifications to the k-ϵ equations presented above as well as the shock-unsteadiness modification developed earlier[5] are applicable only in shock waves. Implementing them in a practical scenario therefore involves identifying the high compression regions in the flowfield. The modifications are then cast in a form such that they are effective only in these regions, and the original model is recovered elsewhere. References 6 and 7 delineate this method by applying the shock-unsteadiness modification to compression ramp and oblique shock wave impinging on a turbulent boundary layer. A similar approach can be followed for the current model. Also, the modifications are strictly valid only when the mean flow is uniform on either side of the shock wave, and the upstream turbulence field is homogeneous. Application to more complex flows may require further modifications and are beyond the scope of this paper.

VI. COMPARISON WITH DNS DATA

We check the efficacy of the new modification introduced in the k-ϵ model by comparing its prediction with DNS data of shock/homogeneous turbulence interaction.[10,12] Of the three cases listed in Table I, the first two are at Mach number 1.29 and the third case is at Mach number 1.5. Case 1.29A has essentially vortical inflow turbulence, while cases 1.29B and 1.5 have an entropic thermodynamic field along with a vortical velocity field upstream of the shock. Morkovin's hypothesis holds in the weak form, i.e., $u_{\rm rms}$ and $T_{\rm rms}$ in the incoming flow satisfy Eq. (1). The cross correlation coefficient $R_{u'T'}$ is given for each case such that

$$\frac{\overline{u'T'}}{\bar{u}\bar{T}} = R_{u'T'}\frac{u_{\rm rms}}{\bar{u}}\frac{T_{\rm rms}}{\bar{T}} = (\gamma-1)M_1^2 R_{u'T'}\frac{\overline{u'^2}}{\bar{u}^2}. \tag{26}$$

The above equation is compared with Eq. (3) to obtain the equivalent A_{uT} for the three cases, and they are listed in Table I. The values of Reynolds number based on the Taylor microscale, Re_λ, and turbulent Mach number, M_t, at the inflow station are also tabulated. These are used to compute the inlet values of k and ϵ_s at $x=0$,

$$k_{in} = M_t^2/2, \tag{27}$$

TABLE I. Mean and turbulent flow quantities for the interaction of homogeneous turbulence with a normal shock. The inflow turbulence is normalized by the upstream values of $\bar{\rho}$, $\tilde{a}$, and $\bar{\mu}$.

Case	M_1	A_{uT}	M_t	Re_λ	k_{in}	ϵ_{in}
1.29A	1.29	0.04	0.14	19.1	9.8×10^{-3}	1.3×10^{-3}
1.29B	1.29	0.56	0.14	19.1	9.8×10^{-3}	1.3×10^{-3}
1.5	1.50	0.82	0.17	6.7	15.0×10^{-3}	4.2×10^{-3}

$$\epsilon_{\mathrm{in}} = 15\frac{\bar{\mu}}{\bar{\rho}}\frac{u_{\mathrm{rms}}^2}{\lambda^2}\frac{L}{a^3} = \begin{cases} \dfrac{5}{3}M_t^4 \ \mathrm{Re}_L/\mathrm{Re}_\lambda^2 & \text{for } M_1 = 1.29 \\ \dfrac{10}{\sqrt{3}}M_t^3/\mathrm{Re}_\lambda & \text{for } M_1 = 1.5. \end{cases} \tag{28}$$

Here, the mean flow variables and k and ϵ are normalized using upstream values of $\bar{\rho}$, $\tilde{a}$, and $\bar{\mu}$, where $\tilde{a}$ is the mean speed of sound and $\bar{\mu}$ is the mean viscosity of the fluid. The reference length scale L in cases 1.29A and 1.29B is chosen such that the Reynolds number based on the reference quantities, Re_L, is 750. Case 1.5 uses a characteristic length of 2λ as reference, where λ is the Taylor microscale as defined in Ref. 16.

The normalized model equations (21) and (22) are integrated through the shock, which is specified as hyperbolic tangent profiles of mean flow quantities. The mean shock thickness is obtained from DNS data. By comparison, the shock thickness obtained by solving the mean flow equations depends on the numerics of the computation and the resolution of the computational grid in the vicinity of the shock wave. The k and ϵ_s amplifications given by Eqs. (21) and (23) are independent of the shock thickness. Therefore the new model results presented below are identical to the solution of the fully coupled mean flow and turbulence model equations. The same is true for the realizable model and the shock-unsteadiness modification results. On the contrary, the standard k-ϵ model predictions are sensitive to the shock thickness, such that the postshock k value and its decay rate increase dramatically when the shock becomes thinner.[5]

The evolution of k obtained by integrating the model equations across the shock wave is plotted in Fig. 11, where the data are normalized by the value of k immediately upstream of the shock. For case 1.29A with negligible upstream entropy fluctuation, the new model is almost identical to the shock-unsteadiness modification proposed by Sinha *et al.*[5] Both models match the k amplification across the shock (at x=2.7) obtained from DNS. The models do not reproduce the rapid variation in k immediately behind the shock ($2<x<2.7$) because they do not model the decay of acoustic energy in this region. Also, the high k values reported by DNS in the shock region are not predicted by the models. These values are an artifact of the unsteady shock motion and do not represent turbulent fluctuations. The standard k-ϵ model and the realizable model results, reproduced from Ref. 5, show a higher value of k downstream of the shock. The above results serve as a baseline for studying the effect of A_{uT}.

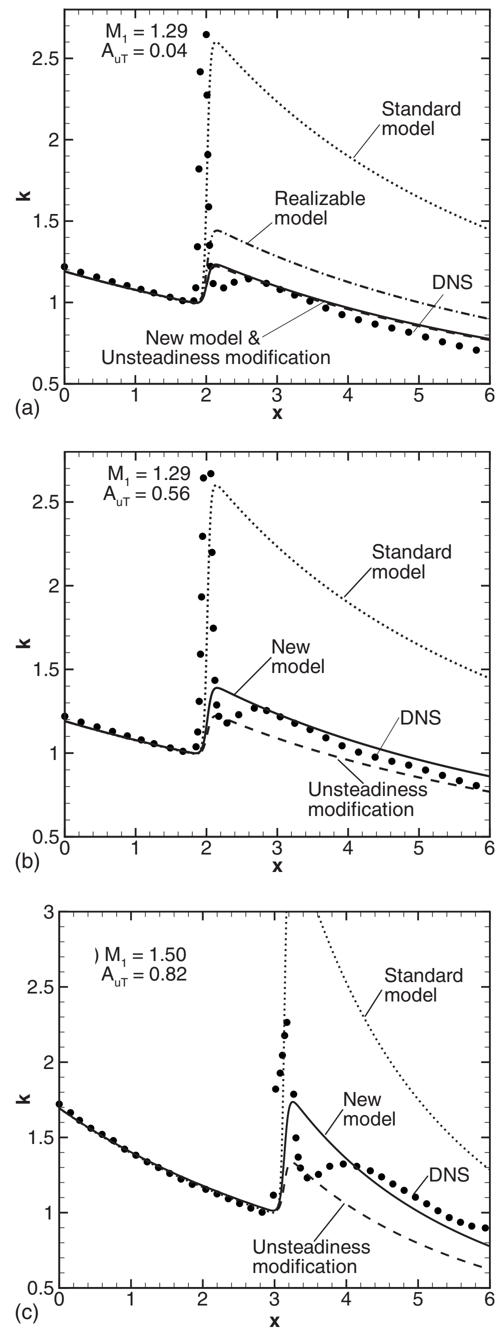

FIG. 11. Evolution of k in the interaction of homogeneous turbulence with a normal shock for cases 1.29A, 1.29B, and 1.5 listed in Table I. Different versions of the k-ϵ models (lines) are compared with DNS data (Refs. 10 and 12) (symbols).

For case 1.29B with $A_{uT}>0$, the new model predicts a higher amplification in turbulent kinetic energy across the shock than case 1.29A. This matches DNS data, for example, at $x\simeq 3$. By comparison, the standard k-ϵ and the shock-unsteadiness model results are insensitive to the variation in A_{uT} and therefore identical to case 1.29A. The realizable model results are also independent of A_{uT} and are not shown in the figure. Downstream of the shock, the current model predicts a slower decay of turbulent kinetic energy as compared to DNS. The same is true for the shock-unsteadiness model and it matches the trend observed at Mach 1.29 in Ref. 5.

At Mach 1.5 and $A_{uT}=0.82$, the new model slightly underpredicts the DNS data downstream of the shock. By comparison, the shock-unsteadiness model results are significantly lower, whereas the standard k-ϵ model grossly overpredicts k amplification across the shock. For this case, $c_{\epsilon 2}=1.5$ is used in the model equation (22). Jamme *et al.*[12] noted that this value of $c_{\epsilon 2}$ matches the turbulence decay rate obtained by their DNS.

VII. CONCLUSIONS

The magnitude of upstream entropy fluctuations and the sign of the velocity-temperature correlation are known to affect the amplification of turbulence across a shock wave. We study the effect of this correlation and its modeling in the RANS framework by considering the interaction of homogeneous turbulence with a normal shock. A parameter A_{uT} is defined to relate the incident velocity and temperature fluctuations. Budget of the turbulent kinetic energy k amplification shows that the primary effect of velocity-temperature correlation comes in via the production due to mean pressure gradient. The source term is positive for negatively correlated velocity and temperature fluctuations $(A_{uT}>0)$ upstream of the shock and has a damping effect for positive correlation $(A_{uT}<0)$. Existing turbulence models do not account for this effect correctly. Linear analysis is used to develop a new physically consistent model for the production due to mean pressure gradient. The shock-unsteadiness parameter and the solenoidal dissipation rate equation developed earlier are also updated to account for the effect of upstream temperature fluctuations. The resulting two-equation model reproduces the enhanced turbulence amplification for $A_{uT}>0$ as well as the damping effect of $A_{uT}<0$. The model predictions match linear theory well for A_{uT} in the range 0–2 but overpredicts the k amplification for higher A_{uT} and for $A_{uT}<0$. The new k-ϵ model is found to reproduce DNS data of shock/homogeneous turbulence interaction well.

ACKNOWLEDGMENTS

The authors wish to thank Professor Krishnan Mahesh of the University of Minnesota for useful discussions and the linear analysis code.

[1] D. Knight, H. Yan, A. Panaras, and A. Zheltovodov, "Advances in CFD prediction of shockwave turbulent boundary layer interactions," Prog. Aerosp. Sci. **39**, 121 (2003).
[2] W. W. Liou, P. G. Huang, and T.-H. Shih, "Turbulence model assessment for shock-wave/turbulent boundary layer interaction in transonic and supersonic flows," Comput. Fluids **29**, 275 (2000).
[3] J. Forsythe, K. Hoffmann, and H.-M. Damevin, "An assessment of several turbulence models for supersonic compression ramp flow," AIAA Paper No. 98-2648, 1998.
[4] T. J. Coakley and P. G. Huang, "Turbulence modeling for high speed flows," AIAA Paper No. 92-0436, 1992.
[5] K. Sinha, K. Mahesh, and G. V. Candler, "Modeling shock unsteadiness in shock turbulence interaction," Phys. Fluids **15**, 2290 (2003).
[6] K. Sinha, K. Mahesh, and G. V. Candler, "Modeling the effect of shock unsteadiness in shock/turbulent boundary layer interactions," AIAA J. **43**, 586 (2005).
[7] A. Ali Pasha and K. Sinha, "Shock-unsteadiness model applied to oblique shock-wave/turbulent boundary layer interaction," Int. J. Comput. Fluid Dyn. **22**, 569 (2008).
[8] P. Bradshaw, "Compressible turbulent shear layers," Annu. Rev. Fluid Mech. **9**, 33 (1977).
[9] P. Martin, "Direct numerical simulation of hypersonic turbulent boundary layers. Part 1. Initialization and comparison with experiments," J. Fluid Mech. **570**, 347 (2007).
[10] K. Mahesh, S. K. Lele, and P. Moin, "The influence of entropy fluctuations on the interaction of turbulence with a shock wave," J. Fluid Mech. **334**, 353 (1997).
[11] K. Mahesh, P. Moin, and S. K. Lele, "The interaction of a shock wave with a turbulent shear flow," Thermosciences Division, Department of Mechanical Engineering, Stanford University, Report No. TF-69, Stanford, CA, 1996.
[12] S. Jamme, J.-B. Cazalbou, F. Torres, and P. Chassaing, "Direct numerical simulation of the interaction between a shock wave and various types of isotropic turbulence," Flow, Turbul. Combust. **68**, 227 (2002).
[13] F. Grasso and D. Falconit, "High-speed turbulence modeling of shock-wave boundary-layer interaction," AIAA J. **31**, 1199 (1993).
[14] D. C. Wilcox, *Turbulence Modeling for CFD*, 2nd ed. (DCW, La Canada, 1998), p. 236.
[15] K. Y. Chien, "Prediction of channel and boundary layer flows with a low Reynolds number turbulence model," AIAA J. **20**, 33 (1982).
[16] H. Tennekes and J. L. Lumley, *A First Course in Turbulence* (MIT, Cambridge, 1972), p. 66.